SCIENTIFIC REPORTS

OPEN

SUBJECT AREAS:
FLUIDS
CHEMICAL PHYSICS

Received
29 August 2013

Accepted
19 November 2013

Published
20 December 2013

Correspondence and requests for materials should be addressed to T.M. (teru@iis.u-tokyo.ac.jp)

An estimation of molecular dynamic behaviour in a liquid using core-loss spectroscopy

Yoshiki Matsui, Koichiro Seki, Akihide Hibara & Teruyasu Mizoguchi

Institute of Industrial Science, the University of Tokyo, Tokyo 153-8505, Japan.

We report an effective approach for estimating the dynamic behaviour of molecules in liquid from their core-loss spectra by combining molecular dynamics simulations and first-principles band-structure calculations. The carbon K-edge of the technologically important methanol was calculated, and the experimental spectra were well reproduced using the presented calculation method, which effectively included multiple-molecule interactions. Several peaks arose from the methanol molecules with different C-O bonding modes, and the splitting of those peaks was sensitively altered by the magnitude of the dynamic behaviour of molecules. These findings allow for estimation of the dynamic behaviour of molecules in liquids using core-loss spectroscopy, and the method offers the potential to identify the dynamic behaviour of the molecules in liquids with high spatial resolution, temporal resolution, and sensitivity.

Liquid is one of the three states of matter with a specific volume but no fixed shape, and is indispensable to modern industry and technology because liquids are widely used as solvents and a large number of chemical reactions take place within liquid media. Given the importance of liquids, their properties, such as dynamic behaviour of molecules in the liquid, have been extensively investigated with infrared (IR) spectroscopy, nuclear magnetic resonance (NMR), X-ray, and neutron scattering as the most widely used techniques. However, to achieve a comprehensive understanding of the chemical reactions, such as catalytic reaction at liquid–solid interfaces, analyses of the liquid properties with improved spatial resolution, temporal resolution, and sensitivity are needed.

Among the existing analytical methods, core-loss spectroscopy using electrons or X-rays, namely electron energy loss near edge structure (ELNES) and X-ray absorption near edge structure (XANES), offers atomic-scale spatial resolution[1,2], nanosecond-level time resolution[3–5], and high sensitivity[6]. Despite the advantages of core-loss spectroscopy, the practical application of this technique in liquid analysis has been limited, largely due to a lack of suitable theoretical methods for calculating the core-loss spectra of liquids. Adequate theoretical calculations are indispensable for interpreting the core-loss spectra.

So far, theoretical calculations of the core-loss spectrum of solid materials have been extensively performed[7]. Generally, the peaks in the spectra of solid materials have been ascribed to static origins such as specific electronic structures and local coordinations. This static interpretation is reasonable for solid materials because their atomic structures are usually rigid. In contrast, the theoretical calculations of liquid spectra are controversial. Although some studies have been performed by combining molecular dynamics (MD) simulations with first-principles cluster calculations[8–10], like those of solid materials, the spectra of liquids have been interpreted in terms of static electronic structures and the local coordination of the molecules[11,12]. Little attention has been paid to the relationship between dynamic molecular behaviours in the liquids and the features of a core-loss spectrum.

In this study, we demonstrated the estimation of the dynamic behaviour of molecules in the liquid by combining the core-loss spectroscopy with the theoretical calculation. Our analysis is based on a consideration for time scales of each phenomenon. The time scale of electron excitation is on the order of sub-femtoseconds ($\sim 10^{-16}$ sec), whereas that of molecular vibrations is on the order of sub-nano- to sub-picoseconds ($10^{-10} \sim 10^{-13}$ sec). Furthermore, the exposure time used to measure the core-loss spectrum is typically much longer, on the order of milliseconds or hours ($10^{-3} \sim 10^{4}$ sec). On the electron-transition time scale, the molecular vibration appears as a (very slow) frame-by-frame advance of snapshots. Thus, interactions between one snapshot and other snapshots can be neglected. In this case, the core-loss spectrum for the liquid should reflect the average spectrum for multiple molecules in the snapshots, and the variety of the molecular structures in the snapshots should be related to the dynamic behaviour of molecules in the liquid. In this study, we combined MD simulations

and first-principles band structure calculations, and extract the dynamic information from the core-loss spectrum.

Results

Methanol was selected as a model because of its relatively simple molecular structure, the availability of experimental spectra, and its importance as a prospective material for use in fuel cells. First, two models were constructed for spectral calculations. The first model included an isolated methanol molecule inside a 10 × 10 × 10-Å box (Fig. 1(b)). The methanol structure was optimised, and this model is hereafter called the 'gas model' because the methanol molecules were separated from each other. The second model, termed the 'liquid model', was constructed from an MD simulation. The validity of the MD simulation was confirmed using simulated melting and boiling temperatures (See Supplementary Information Figure S1). The liquid model at 313 K is shown in Figure 1(c–e).

The periodic boundary conditions were used for the spectral calculations in this study, whereas prior studies used cluster calculations to generate the core-loss spectra of molecules and liquids, and one or several molecules were taken from independent MD calculations[8,9,11,12]. However, as described later, the use of the periodic boundary conditions were important for reproducing the experimental spectra of liquids.

The C K-edge of methanol was calculated for all C atoms in the models, and the calculations of the liquid spectra were performed using different snapshots obtained from the MD simulations at different temperatures. Thus, more than 200 spectral simulations were performed.

The calculated spectra of an isolated methanol molecule using the gas model and that for all methanol molecules in the liquid model are shown in Figure 2. The experimental spectra of gaseous and liquid methanol[13,14] are also shown in Figure 2(q). In the experimental spectra, a clear double peak at the threshold is observed in the spectrum of the gas methanol along with an intense peak (labelled B), whereas the spectrum of liquid methanol shows broad peaks (A and B), and the separation between peaks A and B differs from that of gaseous methanol. The gas-model calculation satisfactorily reproduces the experimental spectrum of gaseous methanol (Fig. 2(q)). The validity of the calculation can be confirmed using the calculated spectrum for larger cell, 12 × 12 × 12Å^3. Furthermore, an MD simulation of the gas model was also performed, and the spectra averaged of 16 and 32 snapshots are shown (Fig. 2(q)). However, the experimental spectrum for liquid methanol was not reproduced well by those gas models; peak B is more intense, and the peak separation between A and B is larger than that observed in the liquid spectrum. Individual calculated spectrum of each molecules in the liquid model is shown in Figs. 2(a–p). It is seen that each molecule generates several different spectral profiles. However, none of the spectra adequately reproduces the experimental spectrum of liquid methanol, indicating that the spectrum of any individual molecular structure cannot reproduce the experimental spectrum of the liquid.

Here, based on the consideration for the time-scales of electron transition, molecular vibration, and exposure time as described above, an average spectrum of the calculated spectra of all methanol molecules in the liquid model was constructed and compared with the experimental data as shown in Figure 3. The profile of the averaged spectrum provides a good reproduction of the experimental

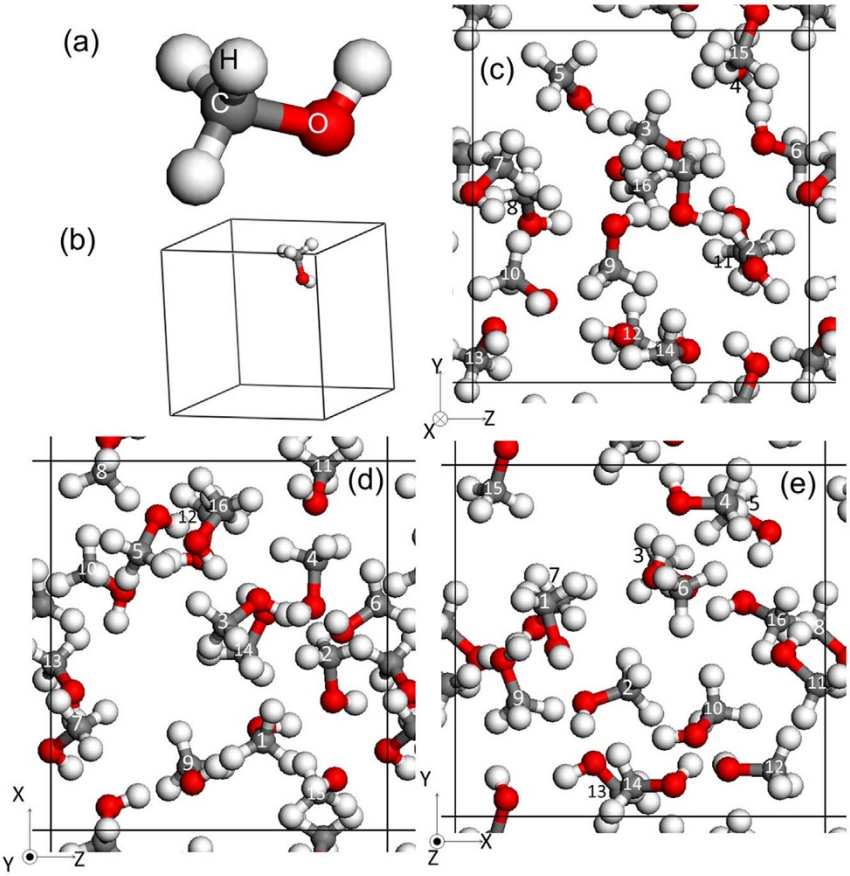

Figure 1 | (a) Optimised structure of the methanol molecule. (b) Gas-state model of methanol using the optimised methanol molecule inside a box-type supercell. (c–e) Liquid model constructed using a molecular dynamics simulation at 313 K view from different orientations. The solid methanol structure was employed as the initial structure for the molecular dynamics simulation, and a snapshot from the molecular dynamics simulation at 313 K was used as the liquid model. The molecules are numbered as shown in the figure.

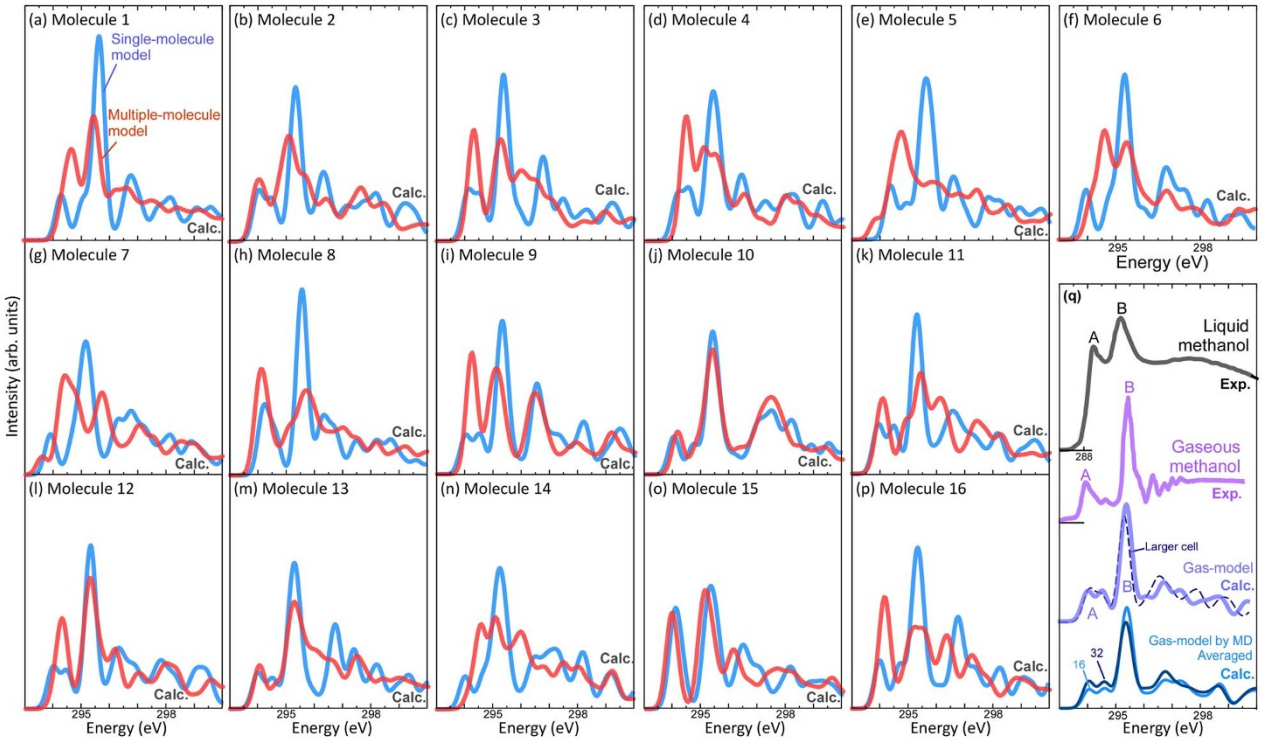

Figure 2 | (a–p) Calculated spectra for the respective methanol molecules in the liquid model; the molecule number corresponds to that in Figure 1(c). The red line indicates the spectrum calculated from the multi-molecule model, whereas the blue line indicates the spectrum from the single-molecule model in which molecules other than the objective molecule were eliminated from the multi-molecule model. (q) Experimental spectra of gaseous and liquid methanol and the calculated spectrum from the gas-models. The experimental spectra were obtained from references[13,14]. In the calculated spectra of the gas-models, the spectrum from the stable molecular structure and the average spectra using 16 and 32 snapshots by the MD simulation of the gas-model were shown.

spectrum of liquid methanol. The reproducibility of the intensity ratio and the separation of peaks A and B, which were not well reproduced by the gas model, were greatly improved in the averaged spectrum.

To confirm the effect of the number of molecules on the averaged spectrum, two other snapshots were acquired from the MD calculations, and their averaged spectra were calculated. The averaged spectra using 16, 32, and 48 methanol molecules are compared in Figure 3. Although the detailed features are slightly smoothed when using a larger number of molecules in the averaged spectrum, the characteristic features such as the intensity ratio and the splitting of peaks A and B remain unchanged, indicating that the outline of the core-loss spectrum of liquid methanol can be reproduced using the average spectrum of ten or several tens of molecules.

Discussion

Here, to confirm the effects of molecule-molecule interactions on the calculated spectrum, model calculations, in which molecules other than the object molecule were eliminated from the liquid model, were performed. This model is hereafter called the 'single-molecule model'. In the single-molecule models, respective molecular structures were identical to those in the liquid model, but no interactions occurred with surrounding molecules. The calculated spectra of the single-molecule models are shown in Fig. 2 with blue lines, and the average spectrum of those single-molecule models is shown in Fig. 3(e). A comparison of the spectra from multi-molecular models (red lines) indicates that each spectrum for a single-molecule model (blue line) differs from that of the multi-molecule models (red lines) (Fig. 2). Furthermore, it is notable that the average spectra for those single-molecule models (Fig. 3(e)) are similar to those of the gas models shown in Fig. 2(q). This indicates that spectral features are influenced by surrounding molecules.

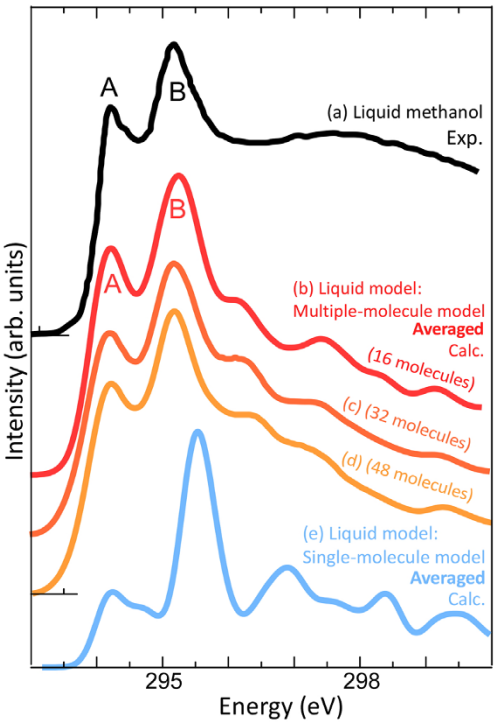

Figure 3 | Experimental spectra of (a) liquid methanol. (b) The average spectrum of the multi-molecule models of the liquid model, which are shown as red lines in Figure 2(a–p). The average spectra of the multiple-molecule models of liquid methanol using (c) 32 and (d) 48 molecules. (e) The average spectrum of the single-molecule models, which are shown as blue lines in Figure 2(a–p).

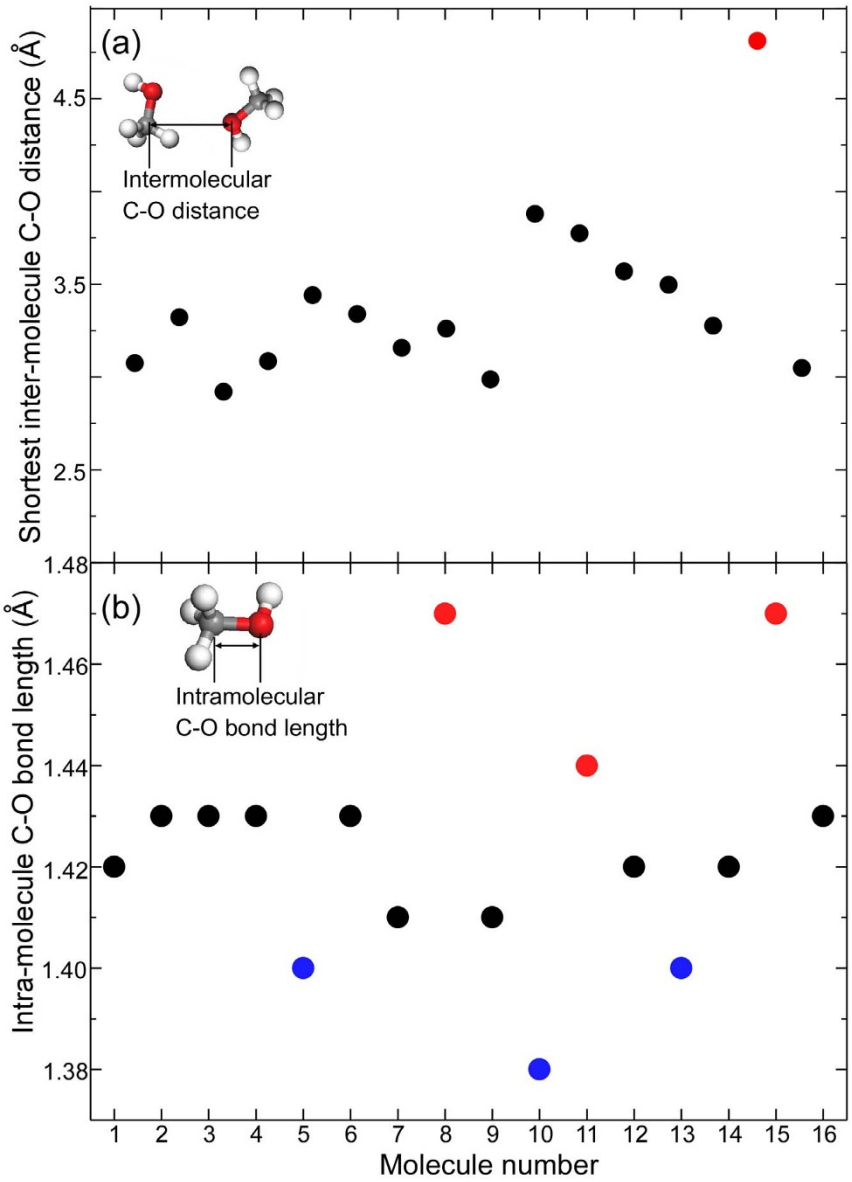

Figure 4 | (a) Intermolecular C-O distance of each methanol molecule. (b) Intramolecular C-O bond length of each methanol molecule. The blue and red circles represent the methanol molecules that have a strong A or B peak, respectively.

To quantify the magnitude of molecule-molecule interactions, intermolecular C-O distances in the multi-molecule model were investigated (Fig. 4(a)). It was found that molecule 15 is separated from the other molecules by approximately 4.8 Å, which is a substantially greater distance than that found for the other molecules. From Fig. 2(o), it is seen that the multi-molecule model (red line) produces a spectrum similar to that of the single-molecule model (blue line). The single- and multi-molecule models spectra are similar to each other in molecule 10 (Fig. 2(j)), whereas these models are slightly different spectra in molecules 11 ~ 13 (Fig. 2(k) ~ (m)), and a clear difference was observed in the case of molecule 14 (Fig. 2(n)). From these results, we can conclude that molecules within a range of approximately 3.5 Å affect the spectral features.

Furthermore, it was also found that the molecule-molecule interactions influence to the atomic configuration of molecules in liquid. The range of intramolecular C–O bond lengths in the liquid models is approximately 1.38 ~ 1.48 Å (Fig. 4(b)), which is much wider than the range of bond lengths in the gas model and the MD simulation of the gas model, 1.40 ~ 1.44 Å. This result indicates that not only the electronic structure but also the atomic coordinations of the molecules are influenced by the molecule–molecule interactions. This result further supports the conclusion that an intermolecular distance much larger than 3.5 Å is indispensable to calculate the liquid spectra.

In previous studies, the spectral calculations of liquids have been performed based on the cluster calculation method using one or a few molecules taken from the MD simulations[8,9,11,12]. However, the present comparison between the single- and multi-molecule models indicates that the presence of molecules around the objective molecule significantly influences the features of the calculated spectrum. Thus, it is concluded that the use of the periodic boundary conditions are important for calculating the spectrum of a liquid.

For the core-loss spectrum of solid materials, the use of one calculated spectrum is usually sufficient for reproducing the experimental spectrum; thus, the peaks in the spectrum originate from the static atomic coordinations and electronic structures. However, for liquids, the use of many spectra from molecules in various environments is necessary for reproducing the experimental spectrum as shown in Figures 2 and 3.

Here, the relationship between the dynamic behaviour of the molecules and their spectral features is discussed by analysing their

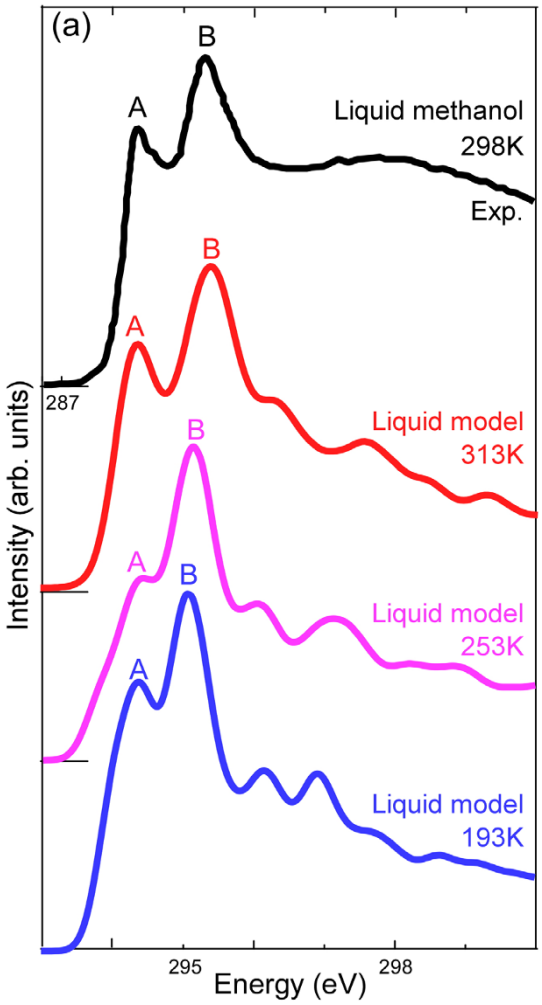

Figure 5 | (Top to bottom) Experimental spectrum of liquid methanol and spectra calculated for 313 K, 253 K, and 193 K. Liquid models were constructed using the molecular dynamics simulations for the respective temperatures. In the present molecular dynamics simulation, methanol is in the liquid state at the given temperatures.

atomic configurations and spectral features. The C–O bond length was selected as a measure to qualitatively represent the magnitude of the molecular dynamic behaviour in the liquid because a general trend was discerned. Figure 4(b) provides a plot of the C-O bond length for each molecule in the liquid model. Molecules 8, 11, and 15 have longer C-O bonds and molecules 5, 10, and 13 have shorter C-O bonds than the other molecules. When revisiting the calculated spectra of the methanol molecules shown in Figure 2, one can see that molecules 8, 11, and 15 share intense peak A, whereas intense peak B instead of peak A is pronounced for molecules 5, 10, and 13. As previously mentioned, molecule 15 is separated from the other molecules. Thus, the pronounced peak A for molecule 15 is primarily due to the long intramolecular C–O bonding. This general trend suggests the possibility that molecules having longer or shorter C-O bonds have a greater influence on peak A or B, respectively. The exceptional cases may be attributed to the influence of the surrounding molecules. Based on this analysis, one can hypothesise that molecules with shorter or longer C-O bonds have a greater contribution to peak A or B, respectively. If this hypothesis is correct, the dynamic behaviour of the molecules in liquid methanol can be estimated based on peaks A and B.

To test this hypothesis, theoretical calculations of the core-loss spectra at different temperatures were performed. Two other liquid models were taken from the 253-K and 193-K MD simulations, and the averaged spectra were calculated. The spectra calculated at different temperatures are compared in Figure 5. Although the overall profiles are similar for each temperature, that is pronounced A and B peaks appear at the threshold followed by a broad C peak, a detailed inspection shows a clear spectral change in which peaks A and B approach one another as the temperature decreases. Figure 6 shows the relationships between the temperature, peak A–B splitting, mean-square displacement (MSD) of all atoms in the supercell, and the averaged changes in C-O bond length during the MD simulations($\Delta L_{C\text{-}O}$), which are commonly related to the magnitude of the dynamic behaviour of molecules. The relative positions of peaks A and B vary proportionally with the temperature, MSD, and $\Delta L_{C\text{-}O}$.

This behaviour can be explained by the previously presented hypothesis, which states that peaks A and B experience greater contributions from molecules with longer and shorter C-O bonds, respectively. At higher temperatures, the molecular vibrations become intense, and molecules of largely varying C-O bond lengths coexist in the liquid. In this case, the electron-electron repulsion becomes stronger with shorter C-O bonding, and peak B is shifted to higher energy. In contrast, the electron-electron repulsion is weakened in longer C-O bonds, and peak A is shifted to lower energy. Thus, the peak A–B splitting increases at higher temperature. In contrast, a narrower distribution of C-O bond lengths is present in the liquid at lower temperatures because molecular vibrations decrease reducing the peak splitting. The predicted value from the calculation well corresponds to the experiment as shown in Figure 6(a).

This direct relationship between the positions of peaks A and B and the dynamic behaviour of molecule is confirmed as shown in Figure 6(b), which enables us to estimate the dynamic behaviour of the constituent liquid molecules, i.e., the molecular vibrations of the molecules in the liquid are more intense for larger A–B peak splitting and weaker for smaller A–B peak splitting.

Through this study, we succeeded in elucidating the relationship between the dynamic behaviour of the molecules in a liquid and its core-loss spectrum. The basis for the dynamic information in the core-loss spectrum is the large differences in time scale for each phenomenon as described above. Although the dynamic information in the core-loss spectrum is smoothed by the averaging of the spectra, we demonstrated that dynamic behaviour is available in the averaged spectrum using suitable spectral calculations.

In summary, an effective method for estimating the dynamic behaviour of molecules in liquids using core-loss spectra was proposed based on a first-principles band structure calculation and an MD simulation. The first two peaks of the C K-edge of methanol are related to the different modes of C-O bonding, and the splitting of these peaks changes with the magnitude of the dynamic behaviour of molecules. The present approach should be applicable to a wide range of liquids. Estimation of such dynamic behaviour in molecules using core-loss spectroscopy enables an in-depth understanding of the properties of a liquid based on high spatial resolution, temporal resolution, and sensitivity. This high-resolution estimation of liquid properties should further facilitate a comprehensive understanding of chemical reactions and their related phenomena in liquids.

Methods

Computational procedures. A $2 \times 2 \times 1$ supercell comprising the unit cell of solid methanol, which contains 16 methanol molecules, was used as the initial structure for the MD simulation[15]. An MD simulation using the empirical force field potential was performed to obtain the liquid structure, and the COMPASS force field[16] was employed in the MD calculations. The time step was set at 0.01 fs, and the simulation time was set to 10 ps. The standard NPT ensemble was used: 1,000,000 steps were simulated at the respective temperatures. The MD simulation conditions were selected to reproduce the experimental properties of methanol, including the melting and boiling points as shown in Fig. S1.

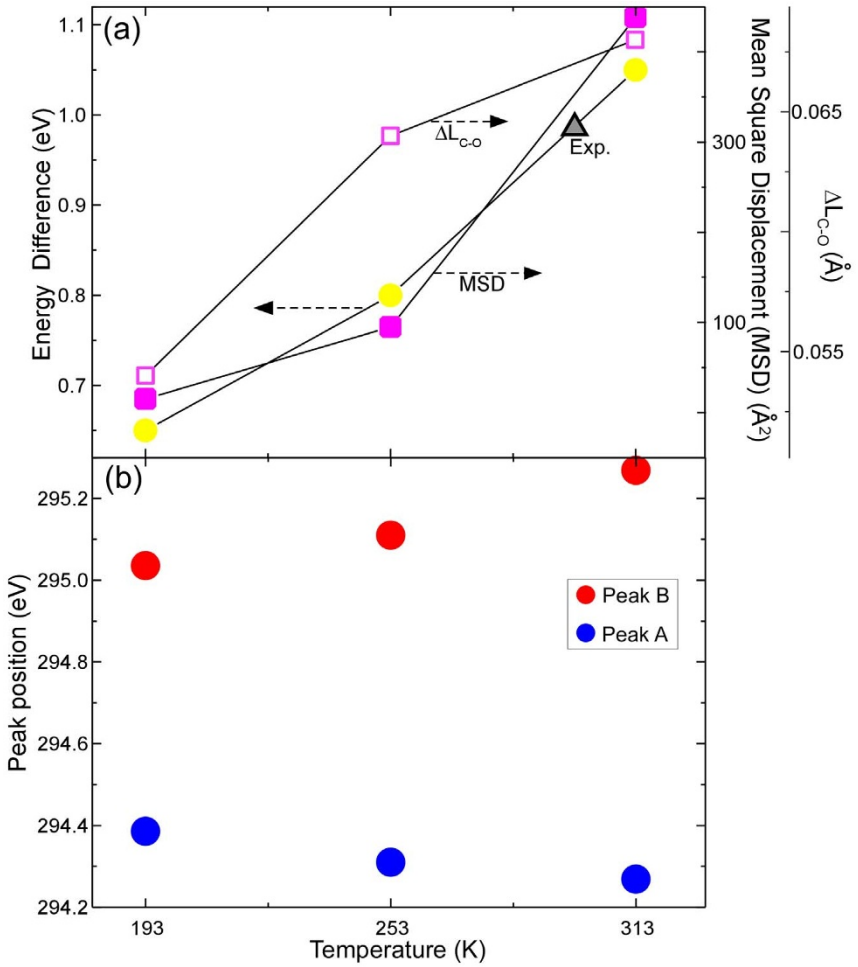

Figure 6 | (a) The relationship among the A–B peak splitting, the mean-square displacement (MSD) of molecules and the averaged changes in C-O bond length during the MD simulations ($\Delta L_{C\text{-}O}$), which are directly related to the magnitude of the molecular vibration and the temperature. A grey triangle shows the experimental value. (b) The position of peaks A and B as a function of the simulated temperature.

The spectral calculations were performed using a first-principles plane-wave basis pseudopotential method (CASTEP code)[17], which was recently applied to calculate the theoretical core-loss spectra (using both ELNES and XANES) for large and complex systems with great success[18–21].

A core-hole effect, which is indispensable for calculating the core-loss spectrum, was taken into account, providing a pseudopotential specially designed for the excited atom with a core hole. The theoretical transition energy was obtained from the total energy difference with a core-orbital correction[20]; using this method, the spectral features and the chemical shifts of the spectrum could be calculated[18–21]. The ELNES calculation with the pseudopotential method described herein is advantageous with respect to the all-electron method because the plane-wave pseudopotential method facilitates an efficient ELNES calculation in large and complex systems. The plane-wave cutoff energy was set to 500 eV, and the core hole was introduced into the carbon 1s orbital.

The aforementioned models based on the isolated methanol molecule and derived from the MD calculation were used in the spectral calculation. A model yielding the object temperature in the MD simulation was selected as the liquid structure providing a snapshot acquired during the MD simulation to calculate the liquid spectra. This assumption has been previously tested and is reasonable because the electron transition process occurs on a faster timescale than the molecular motion[9,11].

1. Jungjohann, K. L., Evans, J. E., Aguiar, J. A., Arslan, I. & Browning, N. D. Atomic-Scale Imaging and Spectroscopy for In Situ Liquid Scanning Transmission Electron Microscopy. *Microsc. Microanal.* **18**, 621–627 (2012).
2. Yoshida, H. *et al.* Visualizing Gas Molecules Interacting with Supported Nanoparticulate Catalysts at Reaction Conditions. *Science* **335**, 317–319 (2012).
3. Iwasawa, Y. In situ characterization of supported metal catalysts and model surfaces by time-resolved and three-dimensional XAFS techniques. *J. Catal.* **216**, 165–177 (2003).
4. LaGrange, T. *et al.* Nanosecond time-resolved investigations using the in situ of dynamic transmission electron microscope (DTEM). *Ultramicroscopy* **108**, 1441–1449 (2008).
5. Zewail, A. H. Four-Dimensional Electron Microscopy. *Science* **328**, 187–193 (2010).
6. Tanaka, I. *et al.* Identification of ultradilute dopants in ceramics. *Nat. Mater.* **2**, 541–545 (2003).
7. Mizoguchi, T., Olovsson, W., Ikeno, H. & Tanaka, I. Theoretical ELNES using one-particle and multi-particle calculations. *Micron* **41**, 695–709 (2010).
8. Cavalleri, M., Ogasawara, H., Pettersson, L. G. M. & Nilsson, A. The interpretation of X-ray absorption spectra of water and ice. *Chem. Phys. Lett.* **364**, 363–370 (2002).
9. Iannuzzi, M. X-ray absorption spectra of hexagonal ice and liquid water by all-electron Gaussian and augmented plane wave calculations. *J. Chem. Phys.* **128**, Artn 204506 (2008).
10. Liang, L., Rulis, P., Ouyang, L. Z. & Ching, W. Y. Ab initio investigation of hydrogen bonding and network structure in a supercooled model of water. *Phys. Rev. B* **83**, Artn 024201 (2011).
11. Cavalleri, M. *et al.* The local structure of protonated water from x-ray absorption and density functional theory. *J. Chem. Phys.* **124**, Artn 194508 (2006).
12. Wernet, P. *et al.* The structure of the first coordination shell in liquid water. *Science* **304**, 995–999 (2004).
13. Nagasaka, M., Hatsui, T., Horigome, T., Hamamura, Y. & Kosugi, N. Development of a liquid flow cell to measure soft X-ray absorption in transmission mode: A test for liquid water. *J. Ele. Spect.* **177**, 130–134 (2010).
14. Kosugi, N., Yamane, H., Nagasaka, M. & Nakane, J. Molecular Inner-Shell Spectroscopy: Local Electronic Structure and Intermolecular Interaction. *Inst. Molec. Sci. Ann. Rev.* 32–33 (2011).
15. Torrie, B. H., Weng, S. X. & Powell, B. M. Structure of the Alpha-Phase of Solid Methanol. *Mol. Phys.* **67**, 575–581 (1989).
16. Sun, H., Ren, P. & Fried, J. R. The COMPASS force field: parameterization and validation for phosphazenes. *Comput. Theor. Polym. S* **8**, 229–246 (1998).
17. Clark, S. J. *et al.* First principles methods using CASTEP. *Z. Kristallogr.* **220**, 567–570 (2005).
18. Gao, S. P., Pickard, C. J., Payne, M. C., Zhu, J. & Yuan, J. Theory of core-hole effects in 1s core-level spectroscopy of the first-row elements. *Phys. Rev. B* **77**, Artn 115122 (2008).

19. Mizoguchi, T., Matsunaga, K., Tochigi, E. & Ikuhara, Y. First principles pseudopotential calculation of electron energy loss near edge structures of lattice imperfections. *Micron* **43**, 37–42 (2012).
20. Mizoguchi, T., Tanaka, I., Gao, S. P. & Pickard, C. J. First-principles calculation of spectral features, chemical shift and absolute threshold of ELNES and XANES using a plane wave pseudopotential method. *J. Phys.: Cond. Mat.* **21**, Artn 104204 (2009).
21. Pickard, C. J., Payne, M. C., Brown, L. M. & Gibbs, M. N. Ab initio EELS with a plane wave basis set. *Inst. Phys. Conf. Ser.* **147**, 211–214 (1995).

Acknowledgments

This work was partially supported by Grant-in-Aid Nos. 22686059, 23656395, and 25106003 from the MEXT and JSPS, JAPAN, and special fund of IIS, Univ. Tokyo (No. 5504850103). Some calculations were performed using supercomputing system in ISSP, Univ. Tokyo. We are gratefully acknowledge to Dr. Chiba in RSI and Dr. A. Chatterjee in Accelrys for helpful discussions.

Author contributions

T.M. supervised this research, directed the calculations and wrote the paper. Y.M. carried out theoretical calculation and data analysis. K.S. and A.H. equally contributed for the discussion on chemical insight of this study.

Additional information

Supplementary information accompanies this paper at http://www.nature.com/scientificreports

Competing financial interests: The authors declare no competing financial interests.

How to cite this article: Matsui, Y., Seki, K., Hibara, A. & Mizoguchi, T. An estimation of molecular dynamic behaviour in a liquid using core-loss spectroscopy. *Sci. Rep.* **3**, 3503; DOI:10.1038/srep03503 (2013).